Coordination Chemistry of Iron Porphycenes in the Presence of CO, CO_2, and *N*-Methylimidazole: Electrochemical, ESR, and UV−Vis Study

C. Bernard,[†] Y. Le Mest,[‡] and J. P. Gisselbrecht*[,†]

Laboratoire d'Electrochimie et de Chimie Physique du Corps Solide, Université Louis Pasteur, UMR CNRS 7512, 4 rue Blaise Pascal, 67000 Strasbourg, France, and Laboratoire de Chimie, Electrochimie Moléculaires et Chimie Analytique, Université de Bretagne Occidentale, UMR CNRS 6521, B.P. 809, 29285 Brest Cedex, France

Received April 24, 1997

The electrochemical behavior of iron porphycenes in benzonitrile, tetrahydrofuran, *N*,*N*-dimethylformamide, and dichloromethane in the presence of Lewis bases is reported. This analysis combined the use of polarographic, steady-state voltammetric, cyclic voltammetric, and spectroelectrochemical methods. Iron(III) 2,7,12,17-tetra-*n*-propylporphycene ([Fe^{III}TPrPn]Cl) is reduced in three one-electron steps and is oxidized in two one-electron steps: All the processes are reversible. The corresponding iron μ-oxo dimer [Fe^{III}TPrPn]$_2$O undergoes four one-electron oxidations as well as four one-electron reductions. [Fe^{III}TPrPn]Cl forms a stable [Fe^{III}TPrPn](N-MeIm)$_2^+$ complex in the presence of N-MeIm. This complex is reduced stepwise to [Fe^{II}TPrPn]N-MeIm, the iron(II) radical anion [Fe^{II}TPrPn$^{\bullet}$]$^-$ and the iron(II) dianion [Fe^{II}TPrPn]$^{2-}$ as confirmed by UV−vis and ESR spectroscopy of the electrogenerated species. In the presence of CO, the reduction of iron(III) generates [Fe^{II}(CO)TPrPn]. In contrast to porphyrins, one- and two-electron reductions of the latter compound are shifted to more negative potentials in DMF and THF and these electron transfers remain reversible. UV−vis spectroelectrochemical experiments at an optically transparent thin layer electrode (OTTLE) demonstrate that the generated species are respectively [Fe^{II}(CO)TPrPn$^{\bullet}$]$^-$ and [Fe^{II}(CO)TPrPn]$^{2-}$. This redox behavior is distinctively different from that of Fe−CO porphyrins. In the presence of CO_2, electrocatalytic reduction of CO_2 is observed, as for porphyrins.

Introduction

Among the seven possible structural isomers of porphyrins, four isomers has been characterized, namely the following: porphycenes, the first known isomer synthesized in 1986,[1,2] corrphycenes, hemiporphycenes, and isoporphycenes,[3−7] the latter being only isolated as a palladium complex. Such a unique series allows studies of changes in physical and chemical properties within structural isomers. Not surprisingly, these fascinating new molecules are attracting considerable interest. The physicochemical properties and specifically the electrochemical behavior of porphyrins have been extensively explored,[8−15] whereas, for porphyrin isomers, only the redox behavior[16−21] and physicochemical[22−29] properties of porphycenes and metalloporphycenes has been examined and remain relatively scarce. The electrochemical behavior of iron porphycenes has been described in a few publications,[19−21] but no study was devoted to the axial coordination ability of iron porphycenes so far. Up to now, the assignment of the electron transfer site (metal versus ligand) for each reduction step of iron porphycenes was only based on UV−vis spectroelectrochemistry and no characterization of the reduced species by ESR spectroscopy has been performed. In the present paper we wish to present a new insight into this assignment of the electron

* To whom correspondence should be addressed.
[†] UMR CNRS 7512.
[‡] UMR CNRS 6521.

(1) Vogel, E.; Köcher, M.; Schmickler, H.; Lex, J. *Angew. Chem., Int. Ed. Engl.* **1986**, *25*, 257−259.
(2) Vogel, E.; Balci, M.; Pramod, K.; Koch, P.; Lex, J.; Ermer, O. *Angew. Chem., Int. Ed. Engl.* **1987**, *26*, 928−931.
(3) Sessler, J. L.; Brucker, E. A.; Weghorn, S. J.; Kisters, M.; Schäfer, M.; Lex, J.; Vogel, E. *Angew. Chem., Int. Ed. Engl.* **1994**, *33*, 2308−2312.
(4) Vogel, E.; Bröring, M.; Weghorn, S. J.; Scholz, P.; Deponte, R.; Lex, J.; Schmickler, H.; Schaffner, K.; Braslavsky, S. E.; Müller, M.; Pörting, S.; Fowler, C. J.; Sessler, J. L. *Angew. Chem., Int. Ed. Engl.* **1997**, *36*, 1651−1654.
(5) Vogel, E.; Bröring, M.; Erben, C.; Demuth, R.; Lex,J.; Nebdel, M.; Houk, K. N. *Angew. Chem., Int. Ed. Engl.* **1997**, *36*, 353−357.
(6) Vogel, E. *Pure Appl. Chem.* **1996**, *68*, 1355−1360.
(7) Vogel, E. *J. Heterocycl. Chem.* **1996**, *33*, 1461−1487.
(8) Boucher, L. J. *Coord. Chem. Rev.* **1972**, *7*, 289−329.
(9) Fuhrhop, J.-H.; Kadish, K. M.; Davis, D. G. *J. Am. Chem. Soc.* **1973**, *95*, 5140−5147.
(10) Giraudeau, A.; Ezahr, I.; Gross, M.; Callot, H. J.; Jordan, J. *Bioelectrochem. Bioenerg.* **1976**, *3*, 519−527.
(11) Felton, R. H. In *The Porphyrins*; Dolphin, D., Ed.; Academic Press: New York, 1978; Vol. 5, Chapter 3, pp 53−125.
(12) Giraudeau,A.; Callot, H. J.; Jordan, J.; Ezhar, I.; Gross, M. *J. Am. Chem. Soc.* **1979**, *101*, 3857−3862.
(13) Kadish, K. M. In *Iron Porphyrins*; Lever, A. B. P., Gray, H. B., Eds; Addison Wesley: Reading, MA, 1983; Part 2, pp 161−249.
(14) Kadish, K. M. In *Progress in Inorganic Chemistry*; Lippard S. J., Ed.; John Wiley & Sons: New York, 1986; Vol. 34, pp 435−605.
(15) Guilard, R.; Lecomte, C.; Kadish, K. M. *Structure and Bonding*; Springer Verlag: Berlin, Heidelberg, 1987; Vol. 64, pp 205−268.
(16) Renner, M. W.; Forman, A.; Wu, W.; Chang, C. K.; Fajer, J. *J. Am. Chem. Soc.* **1989**, *111*, 8618−8621.
(17) Gisselbrecht, J. P.; Gross, M.; Köcher, M.; Lausmann, M.; Vogel, E. *J. Am. Chem. Soc.* **1990**, *112*, 8618−8620.
(18) Kadish, K. M.; Van Caemelbecke, E.; Boulas, P.; Dsouza, F.; Vogel, E.; Kisters, M.; Medforth, C. J.; Smith K. M. *Inorg. Chem.* **1993**, *32*, 4177−4178.
(19) Kadish, K. M.; D'Souza, F.; Boulas, P.; Van Caemelbecke, E.; Vogel, E.; Aukauloo, M. A.; Guilard, R.; Lausmann, M. *Inorg. Chem.* **1994**, *33*, 4474−4479.
(20) Kadish, K. M.; Boulas, P.; D'Souza, F.; Aukauloo, M. A.; Guilard, R.; Lausmann, M.; Vogel, E. *Inorg. Chem.* **1994**, *33*, 471−476.
(21) Bernard, C.; Gisselbrecht, J. P.; Gross, M.; Vogel, E.; Lausmann, M. *Inorg. Chem.* **1994**, *33*, 2393−2401.

S0020-1669(97)00472-2 CCC: $15.00
Published on Web 01/07/1998

transfer site and to report unexpected results on axial coordination of iron in porphycenes.

Because of the importance of axial coordination in iron porphyrins in their biological functions, we were interested in the consequences of the changes from porphyrin to porphycene on the physicochemical properties of iron complexes. The reactivity of iron porphyrins toward Lewis bases like N-MeIm[30−32] and CO[33,34] has been studied extensively. As well, because the direct electrochemical reduction of CO_2 requires very negative potentials,[35−37] extensive efforts have been devoted to the search of catalysts capable of decreasing this overpotential. Transition metal complexes of tetraazamacrocycles,[38,39] bipyridine,[40] and tetrapyrrolic macrocycles such as phtalocyanines[41] and tetraphenylporphyrins[42] were found to act as good catalysts. A first goal for us was to establish whether iron porphycenes are able to catalyze the reactions as well. The present paper also deals with the redox characteristics of iron(III) 2,7,12,17-tetra-*n*-propylporphycene ([Fe^{III}TPrPn]Cl) (Chart 1) in the absence and presence of the Lewis bases *N*-methylimidazole (N-MeIm) and CO. As well the redox behavior of the μ-oxo dimer is compared to that of porphyrins. To characterize the various reduction stages of the iron porphycenes by ESR spectroscopy and UV-vis spectrophotometry, bulk electrochemical studies were carried out under strictly anhydrous and O_2-free media.

Chart 1. Studied Iron Porphycenes

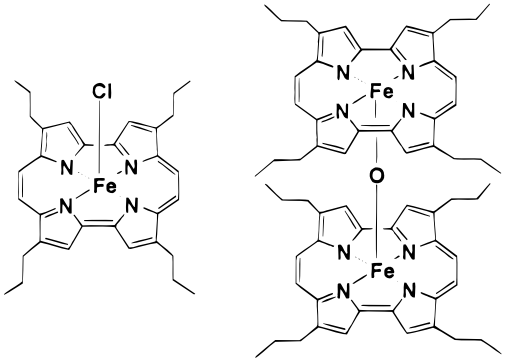

[Fe(III)TPrPn]Cl [Fe(III)TPrPn]$_2$O

Experimental Section

Iron(III) 2,7,12,17-tetra-*n*-propylporphycene and the corresponding μ-oxo dimer (Chart 1) used in the present study were synthesized in accord with published procedures.[1,2,43] Their electrochemistry was studied in four different solvents: *N*,*N*-dimethylformamide (DMF), tetrahydrofuran (THF), dichloromethane (CH_2Cl_2), and benzonitrile (PhCN). All four of these afforded acceptable porphycene solubility. Due to the high sensitivity of the reduced species toward traces of oxygen and water, bulk electrolysis and ESR experiments were carried out in benzonitrile in a drybox with carefully deoxygenated solvents and chemicals.

Chemicals. Tetraethylammonium perchlorate (TEAP from Fluka) was used as the supporting electrolyte in DMF. It was recrystallized before use.[44] For the studies carried out in CH_2Cl_2 and in THF, tetrabutylammonium perchlorate (TBAP from Fluka) was used as the supporting electrolyte. It was purified according to standard procedures.[45]

The solvents were purified according to the following procedures. DMF (Fluka) was purified as described previously[45] and stored under argon. CH_2Cl_2 (sds) was dried over molecular sieves (4 Å), stored under argon, and distilled from CaH_2 before use. THF (sds) was purified by distillation from $LiAlH_4$ immediately before use. PhCN used for bulk electrolysis as a hyper dry medium was purified as described previously and stored in a glovebox.[46]

High-purity CO_2 (99.99%) and CO (99%) gases were used without any further purification. The solubility of CO_2 in CH_2Cl_2 was measured by addition of excess standard 0.02 mol/L $Ba(OH)_2$ solution and back-titration with standard 0.02 mol/L oxalic acid (Merck) using phenolphthalein as indicator.[47] The solubility of CO_2 in CH_2Cl_2 was found to be 0.014 mol/L in agreement with previous studies.[35,36] Partial CO_2 pressures were achieved by mixing known gas flows of argon and CO_2 through the studied solution for at least 5 min.

Apparatus. Reductions were achieved either chemically with sodium amalgam or electrochemically through controlled potential electrolysis; in the latter case, a small electrolysis cell (0.5 mL of electrolyte solution) was used and the working electrode was a platinum rotating disk electrode (4 mm diameter). The auxiliary electrode and the reference electrode (ferrocenium/ferrocene (Fc^+/Fc)) were separated from the electrolysis cell by a glass frit of low porosity (Vycor tips from PAR). The cell was connected to a potentiostat (PAR Model 173) equipped with a PAR 179 digital coulometric unit and monitored by a PAR 175 programmer. Using a 2 mm diameter platinum electrode, the apparatus was also used to carry out RDE and low sweep rate CV measurements.

Steady state voltammetry on a rotating disk electrode (RDE) and cyclic voltammetry (CV) with sweep rates ranging from 10 mV/s to 20 V/s were carried out on a computerized electrochemical device DACFAMOV (Microtec-CNRS, Toulouse, France) connected to an Apple II microcomputer. A classical three-electrode cell was used.

(22) Ofir, H.; Regev, A.; Levanon, H.; Vogel, E.; Köcher, M.; Balci, M. *J. Phys. Chem.* **1987**, *91*, 2686−2688.
(23) Levanon, H.; Toporowicz, M.; Ofir, H.; Fessenden, R. W.; Das, P. K.; Vogel, E.; Köcher, M.; Pramod, K. *J. Phys. Chem.* **1988**, *92*, 2429−2433.
(24) Schlüpmann, J.; Huber, M.; Toporowicz, M.; Köcher, M.; Vogel, E.; Levanon, H.; Möbius, K. *J. Am. Chem. Soc.* **1988**, *110*, 8566−8567.
(25) Schlüpmann, J.; Huber, M.; Toporowicz, M.; Plato, M.; Köcher, M.; Vogel, E.; Levanon, H.; Möbius, K. *J. Am. Chem. Soc.* **1990**, *112*, 6463−6471.
(26) Vogel, E. *Pure Appl. Chem.* **1990**, *62*, 557−564.
(27) Wehrle, B.; Limbach, H. H.; Köcher, M.; Ermer, O.; Vogel, E. *Angew. Chem., Int. Ed. Eng.* **1987**, *26*, 934−936.
(28) Oertling, W. A.; Wu, W.; Lopez-Garriga, J. J.; Kim, Y.; Chang, C. K. *J. Am. Chem. Soc.* **1991**, *113*, 127−134.
(29) Waluk, J.; Müller, M.; Swiderek, P.; Köcher, M.; Vogel, E.; Hohlneicher, G.; Michl, J. *J. Am. Chem. Soc.* **1991**, *113*, 5511−5527.
(30) Walker, F. A.; Lo, M. W.; Ree, M. T. *J. Am. Chem. Soc.* **1976**, *98*, 5552−5560.
(31) Quinn, R.; Nappa, M.; Valentine, J. S. *J. Am. Chem. Soc.* **1982**, *104*, 2588−2595.
(32) Geiger, D. K.; Pavlak, E. J.; Kass, L. T. *J. Chem. Educ.* **1991**, *68*, 337−339.
(33) Geutin, C.; Lexa, D.; Momenteau, M.; Savéant, J. M. *J. Am. Chem. Soc.* **1990**, *112*, 1874−1880.
(34) Balducci, G.; Chottard, G.; Geutin, C.; Lexa, D.; Savéant, J. M. *Inorg. Chem.* **1994**, *33*, 1972−1978.
(35) Eggins, B. R.; McNeill, J. *J. Electroanal. Chem.* **1983**, *148*, 17−24.
(36) Croisy, A.; Lexa, D.; Momenteau, M.; Savéant, J. M. *Organometallics* **1985**, *9*, 1574−1579.
(37) Amatore, C.; Nadjo, L.; Savéant, J. M. *Nouv. J. Chim.* **1984**, *8*, 565−566.
(38) Beley, M.; Collin, J. P.; Ruppert, R.; Sauvage, J. P. *J. Chem. Soc., Chem. Commun.* **1984**, 1315−1316.
(39) Beley, M.; Ruppert, R.; Sauvage, J. P. *J. Am. Chem. Soc.* **1986**, *108*, 7461−7467.
(40) Bruce, M. R. M.; Megehee, E.; Sullivan, B. P.; Thorp, H. H.; O'Toole, T. O.; Downard, A; Pugh, J. R.; Meyer, T. J. *Inorg. Chem.* **1992**, *31*, 4864−4873.
(41) Lieber, C. M.; Lewis, N. S. *J. Am. Chem. Soc.* **1984**, *106*, 5033−5034.
(42) Hammouche, M.; Lexa, D.; Savéant, J. M. *J. Electroanal. Chem.* **1988**, *249*, 347−351.
(43) Lausmann, M.; Zimmer, I.; Lex, J.; Lueken, H.; Wiegard, K.; Vogel, E. *Angew. Chem., Int. Ed. Engl.* **1994**, *33*, 736−739.
(44) Callot, H. J.; Giraudeau, A.; Gross, M. *J. Chem. Soc., Perkin Trans. 2* **1975**, 1321−1324.
(45) El Jammal, A.; Graf, E.; Gross, M. *Electrochim. Acta* **1986**, *11*, 1457−1465.
(46) Le Mest, Y.; L'Her, M.; Hendricks, N. H.; Kim, K.; Collman, J. P. *Inorg. Chem.* **1992**, *31*, 835−847.
(47) Eggins, B. R.; McNeill, J. *J. Electroanal. Chem.* **1983**, *148*, 17−24.

The working electrode was either a platinum disk electrode (2 mm diameter EDI type, Tacussel, France) or a glassy carbon electrode (GCE 3 mm diameter). The auxiliary electrode was a platinum wire, and the reference electrode was an aqueous saturated calomel electrode. In our studies ferrocene was used as the internal standard. The Fc^+/Fc redox couple ($E_{1/2}$) was observed at +0.48 V/SCE in CH_2Cl_2 + 0.1 M TBAP, +0.49 V/SCE in DMF + 0.1 M TEAP, and +0.55 V/SCE in THF + 0.1 M TBAP, respectively.

Spectroelectrochemical experiments were carried out with a diode array spectrophotometer (Hewlett Packard 8452 A). The spectroelectrochemical cell was a homemade borosilicate glass cell having an optical pathway of about 0.1 mm. The optical transparent thin layer electrode (OTTLE) was a platinum grid (1000 mesh) placed in the optical pathway. Under these conditions an exhaustive electrolysis was carried out in a few minutes (5 min) instead of 0.5 h for a large-scale electrolysis. As a result of this shorter time scale, further chemical reactions of the electrogenerated species were avoided and spectral measurements were possible on the species resulting from the electron transfer reactions.

ESR measurements were carried out on a JEOL FE3X spectrometer, and spectra were recorded from solutions ($v = 50\ \mu$L) in quartz tubes; the power was 1 mW, and the frequency was close to 9.2 GHz. Spectra were typically run at 140 K by using a flowing nitrogen controller.

The drybox used to carried out bulk electrolysis prior to ESR studies was manufactured by Jaram: The nitrogen flow was continuously purified by passing through molecular sieves at room temperature and divided copper BTS catalyst (BASF) at 100 °C.

Results

Electrochemical Behavior of [Fe^{III}TPrPn]Cl. The redox properties of the mononuclear iron(III) tetrapropylporphycene have been studied previously[21] using a combination of standard cyclic voltammetry and OTTLE-type absorption spectroscopy. RDE experiments and cyclic voltammetry of [Fe^{III}TPrPn]Cl exhibit five distinct one-electron redox steps in CH_2Cl_2 and in PhCN, three reductions and two oxidations, illustrated in Figure 1. Their characteristics are summarized in Table 1.

It has been shown[21] that stepwise reductions of [Fe^{III}TPrPn]Cl in an OTTLE lead to well-defined spectral patterns. Each reduction step exhibits absorption spectra with well-resolved isosbestic points. When compared with those observed for free-base porphycenes and for other metallo(II) porphycenes, the observed spectra were considered consistent with the following reduction scheme:[21]

$$[Fe^{III}TPrPnCl] \overset{e^-}{\rightleftharpoons} [Fe^{II}TPrPn] \overset{e^-}{\rightleftharpoons} [Fe^{II}TPrPn^{\bullet}]^- \overset{e^-}{\rightleftharpoons} [Fe^{II}TPrPn]^{2-}$$

Bulk electrolysis of [Fe^{III}TPrPn]Cl at the plateau potential of the first reduction step **(**reduction of Fe(III) to Fe(II)) yield in DMF, THF, or CH_2Cl_2 the corresponding iron μ-oxo porphycene dimer.[21] It was identified by its UV−vis absorption spectrum and its electrochemical behavior. Thus, under the experimental conditions of this exhaustive coulometry, traces of oxygen in the solution precluded the generation of any observable monomeric iron(II) species.

For this reason we have performed coulometric reductions in an O_2- and H_2O-free atmosphere box and in strictly anhydrous medium, namely PhCN + 0.1 M (TBA)PF_6 dried on activated alumina. In these drastic conditions, it was possible to generate electrochemically pure solutions of the one-electron and the two one-electron reduced species of iron(III) porphycene. The electrogenerated one-electron and two-electron reduced species are stable for hours and, as documented in Figure 1b, give by RDE voltammetry respectively one oxidation wave after a 1 *F*/mol reduction and two oxidation waves after a 2 *F*/mol reduction. These oxidation waves have the same amplitude and half-wave potentials as the corresponding reduction waves for [Fe^{III}TPrPn]Cl before electrolysis. This behavior indicates that the involved redox processes are reversible on the time scale of coulometry and that the generated species do not undergo noticeable degradation.

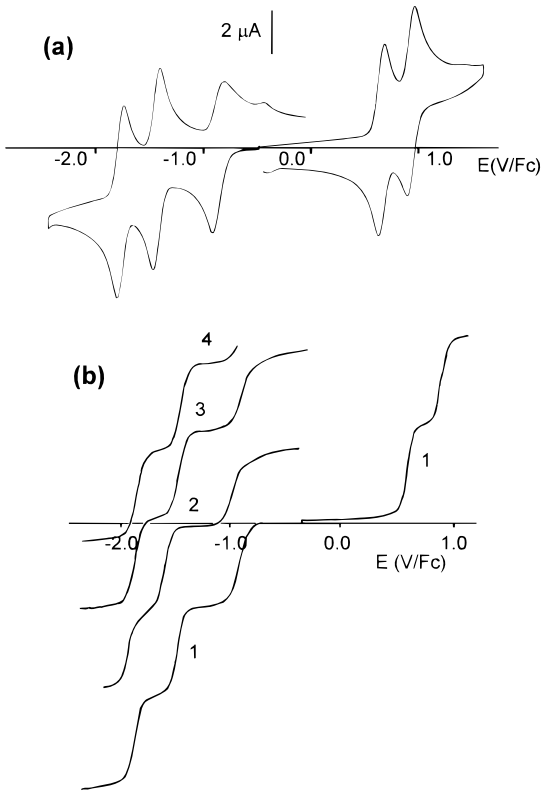

Figure 1. Redox behavior of $[FeTPrPn]^+$ in dry PhCN + 0.1 M (TBA)PF_6: (a) Cyclic voltammetry on Pt at 0.1 Vs^{-1}. (b) RDE on Pt at 2000 rpm of (1) $[FeTPrPn]^+$, (2) after electrolysis at −1.3 V/Fc (1 *F*/mol), (3) after electrolysis at −1.6 V/Fc (2 *F*/mol), and (4) after electrolysis at −2.1 V/Fc (2.7 *F*/mol).

Table 1. Formal Redox Potentials (in V vs Fc^+/Fc) of [FeTPrPn]Cl in PhCN and CH_2Cl_2

solvent	2nd oxid	1st oxid	1st redn	2nd redn	3rd redn
PhCN	+0.93	+0.66	−0.86	−1.44	−1.77
CH_2Cl_2	+0.90	+0.67	−0.80	−1.39	−1.71

Even in these conditions, the preparation of a pure solution of the three-electron reduced species failed. However the three-electron reduced species could be generated as a mixture with the two-electron reduced form (ratio 3−/2− ca. 0.7/0.3) as indicated by the anodic−cathodic third wave by RDE voltammetry (Figure 1b).

The localization of the charge (metal versus ring) and the spin state of the different species, i.e. [Fe^{III}TPrPn]Cl, [Fe^{II}TPrPn], $[FeTPrPn]^-$, and $[FeTPrPn]^{2-}$, in the pure solvent could be analyzed by ESR spectroscopy and are discussed below.

The electrochemical oxidation of [Fe^{III}TPrPn]Cl was also studied in dry PhCN. Under OTTLE conditions, the spectrum of the species generated by the first oxidation (Figure 2a) was similar to the spectra observed for free-base or metalloporphycene radical cations.[21] These observations indicate that the generated species is likely the radical cation i.e. $[Fe^{III}TPrPn^{\bullet}]^+$. Moreover, studies of a series of iron(III) porphycenes with different axial anionic ligands (XFeTPrPn, where X = Cl, Br,

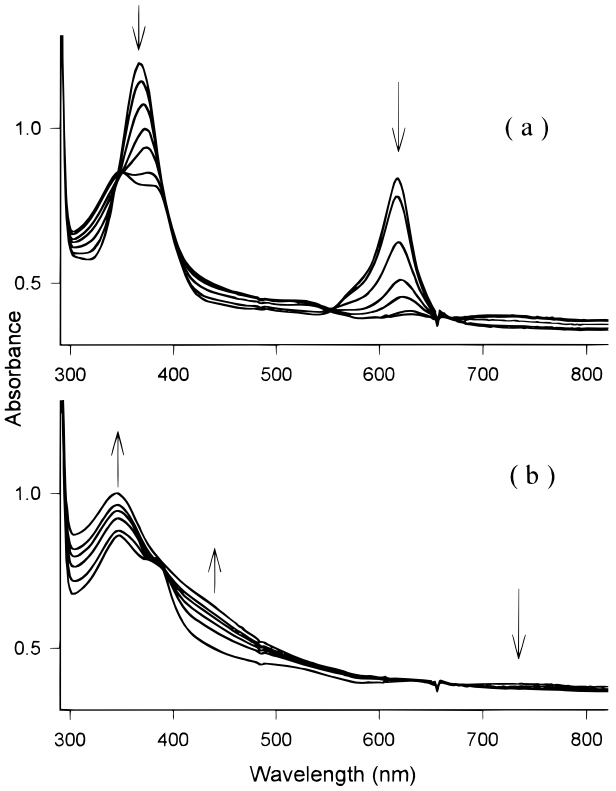

Figure 2. Time-resolved UV−vis absorption spectra of $[FeTPrPn]^+$ in PhCN + 0.1 M $(TBA)PF_6$ on a Pt OTTLE: (a) First one-electron oxidation (electrolysis at +0.8 V/Fc); (b) second one-electron oxidation (electrolysis at +1.1 V/Fc).

and N_3)[48] showed that the first oxidation potential was not influenced by axial ligation of the iron. Such a behavior is an additional indication of a ligand-centered oxidation process.[49] The species generated by the second oxidation (Figure 2b) also displays the pattern of a ligand-centered oxidized species.[21] It should be noted that, even in dry medium, this species is not very stable and the initial spectrum could not be fully regenerated through reduction.

Redox Behavior of [Fe^{III}TPrPn]Cl in the Presence of N-MeIm. Nitrogen-containing Lewis bases are well-known to axially coordinate iron(III) and iron(II) porphyrins.[30−32] The ligand/metal stoichiometry is usually determined by spectroscopy and, for iron(III) porphyrins, is a 2/1 stoichiometry.

The N-MeIm/Fe^{III}TPrPn stoichiometry in DMF was determined through UV−vis spectroscopy. The UV−vis spectra of [FeTPrPn]Cl were recorded with increasing amounts of N-MeIm added to the iron porphycene solution. The spectral changes are shown in Figure 3. The spectral absorbency evolution at 614 nm clearly confirms the coordination of 2 N-MeIm per $[Fe^{III}TPrPn]^+$. In the case of porphyrins, the spectrum of the 2/1 complex (N-MeIm/Fe) is observed only with a large excess of ligand.[30] The present results indicate that iron(III) porphycene binds N-MeIm more strongly than iron porphyrins, as confirmed hereafter. As the spectrum does not change anymore after a 2-fold addition of N-MeIm, the determination of the stability constant could not be achieved by spectroscopy.

Under these conditions, the shift in reduction potential accompanying the binding of axial ligands allows the determination of the stoichiometry and of the axial ligand formation

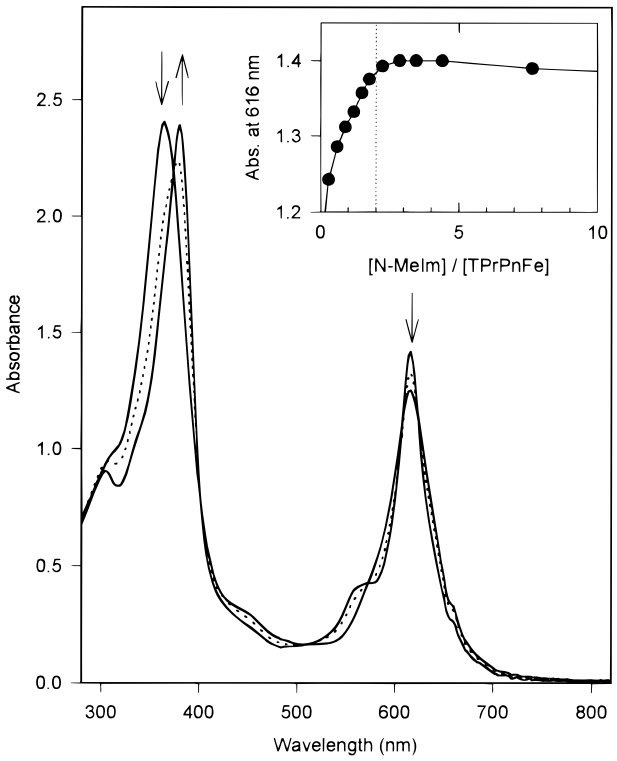

Figure 3. Evolution of the UV−vis spectra of $[FeTPrPn]^+$ in DMF in the presence of increasing amounts of N-MeIm. Insert: Evolution of the Q band absorbance at 416 nm as a function of the ratio N-MeIm/$[FeTPrPn]^+$.

constants corresponding to the different oxidation states of iron porphycene in the presence of increasing amounts of N-MeIm. To determine the stoichiometry changes occurring during the reduction processes, as well as the stability constants of N-MeIm with iron, we ran the cyclic voltammetry of $[Fe^{III}TPrPn]^+$ for different N-MeIm concentrations. The Stackelberg equation[50] relates the half-wave reduction potentials to the axial ligand complexation constants of iron porphycene for each reduction step, where $(E_{1/2})_c$ and $(E_{1/2})_s$ are half-wave potentials in the

$$(E_{1/2})_c = (E_{1/2})_s - 0.059 \log(K_p^{ox}/K_q^{red}) - 0.059 \log[\mathbf{L}]^{p-q} \quad (1)$$

presence and the absence of ligand **L**, respectively, and p and q are the number of ligands **L** bound to the oxidized and reduced species. K_p^{ox} is the stability constant of the oxidized species coordinated to p ligands **L**, and K_q^{red} the stability of the reduced species coordinated to q ligands **L**.

If two steps of axial ligand addition are possible for iron(III) porphycene, the first step is the formation of the 1/1 complex

$$FePn + L \overset{K_1}{\rightleftharpoons} FeLPn$$

and the second step is the formation of the 2/1 complex

$$FeLPn + L \overset{K_2}{\rightleftharpoons} FeL_2Pn$$

Our studies were carried out in DMF + 0.1 M $(TBA)PF_6$. Among the three reduction steps of $[Fe^{III}TPrPn]Cl$, only the first two were shifted toward more negative potentials for increasing concentrations of N-MeIm. The plot of E versus log [N-MeIm]

(48) Lausmann, M. Unpublished results, Ph.D. Dissertation, Köln, 1993.
(49) Phillippi, M. A.; Shimomura, E. T.; Goff, H. M. *Inorg. Chem.* **1981**, *20*, 1322−1325.
(50) Bard, A. J.; Faulkner, L. R. *Electrochemical Methods*; John Wiley & Sons: New York, 1980; Chapter 5.

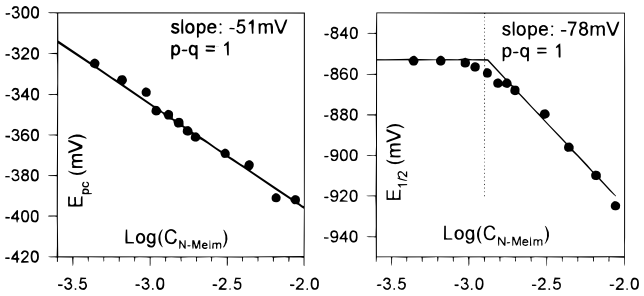

Figure 4. Evolution of the redox potential of the first (a) and second (b) reduction of $[FeTPrPn]^+$ ($c = 4.4 \times 10^{-4}$ mol L^{-1}) with increasing amounts of N-MeIm.

for both reductions (Figure 4) gave a line with a slope of −51 mV characteristic of the loss of one N-MeIm during the first reduction step ($p - q = 1$ in relation 1). Two lines were observed for the second reduction step. For less than stoichiometric amounts of N-MeIm, no change occurred ($p - q = 0$) whereas for higher concentrations we obtained a line with a −78 mV slope. Despite a higher slope than the expected 59 mV, this value is indicative of loss of one N-MeIm during the second reduction step ($p - q = 1$). The third reduction step remained at a constant potential typical for an unchanged coordination number of N-MeIm ($p - q = 0$) during reduction. Such a behavior is expected since iron(III) binds only two N-MeIm which are lost stepwise so that the two-electron reduced species does not bind anymore N-MeIm. This was confirmed by spectroelectrochemical measurements as described below.

Spectroelectrochemical studies were performed on a platinum OTTLE cell to characterize the generated species. For each reduction step, spectral changes with well-defined isosbestic points were observed and the initial species could be recovered through stepwise reoxidations. The absorption bands of [Fe^{II}-TPrPn] in the presence and absence of N-MeIm are different. In the absence of N-MeIm, the absorption bands occur at 342 (sh), 366 (Soret band), 575 (sh), 610, and 622 nm, whereas, in the presence of N-MeIm, the absorption bands are at 344 (sh), 376 (Soret band), 568, and 622 nm (broad band). After the two one-electron reductions of $[Fe^{III}TPrPn]^+$, the observed spectra were identical in both conditions and are characteristic of $[Fe^{II}TPrPn^{\bullet}]^-$, which confirms that the latter species does not coordinate N-MeIm.

The observed redox and spectral data, in the presence of N-MeIm, are in agreement with the following stoichiometric changes occurring during the stepwise reduction of [Fe^{III}TPrPn]-(N-MeIm)$_2$ and are given in the following scheme:

$$[Fe^{III}TPrPn]^+(\text{N-MeIm})_2 \overset{+e^-,\ -\text{N-MeIm}}{\rightleftharpoons} [Fe^{II}TPrPn](\text{N-MeIm}) \overset{+e^-,\ -\text{N-MeIm}}{\rightleftharpoons} [Fe^{II}TPrPn^{\bullet}]^-$$

As the two-electron reduced species does not bind any ligand, relation (1) applied to the second reduction wave of [Fe^{III}-TPrPn]$^+$ with $q = 0$ reduces to

$$(E_{1/2})_c = (E_{1/2})_s - 0.059 \log K_1^{ox} - 0.059 \log [\mathbf{L}] \quad (2)$$

from which $K_1^{ox} = |[Fe^{II}TPrPn](\text{N-MeIm})|/(|[\text{N-MeIm}]||[Fe^{II}$-TPrPn]|), the stability constant of [Fe^{II}TPrPn]N-MeIm, can be extracted. The value of $(E_{1/2})_c$ according to relation (2) is given from the *y* intercept of the linear part of the curve *E* versus log [N-MeIm]. This leads to $K_1^{ox} = 4.0 \times 10^3$. Relation (1) applied to the first reduction step of $[Fe^{III}TPrPn]^+$ with $p = 2$ and $q = 1$ becomes

$$(E_{1/2})_c = (E_{1/2})_s - 0.059 \log(K_2^{ox}/K_1^{red}) - 0.059 \log [\mathbf{L}] \quad (3)$$

where $K_2^{ox} = |[Fe^{III}TPrPn]^+(\text{N-MeIm})_2|/(|[\text{N-MeIm}]|\ |[Fe^{II}$-TPrPn](N-MeIm)|) allowed us to calculate log K_2^{ox} after determination of the *y* intercept of the linear portion of the curve and reporting the above calculated stability constant $K_1^{ox} = K_1^{red}$. This method gave $K_2^{ox} = 7.9 \times 10^6$ for the binding constant of two N-MeIm to $[Fe^{III}TPrPn]^+$ in DMF.

Compared to porphyrins the result shows that $[Fe^{III}TPrPn]^+$ binds N-MeIm more strongly ($\beta_2 = K_1K_2 = 3.2 \times 10^{10}$) than $[Fe^{III}TPP]^+$ ($\beta_2 = 6 \times 10^4$)[30] and also that the generated [Fe^{II}-TPrPn] binds only one N-MeIm. Such a result in not unusual[32,51,52] but is seldom seen for iron(II) porphyrins. Due to the smaller size of the porphycene cavity compared to porphyrins, it is not excluded that iron(II) lies out of the plan so that a second strong coordination is excluded. However due to the lack of any crystallographic structure of iron(II) porphycene, this hypothesis cannot be discussed.

The electrogenerated reduced species in the presence of added N-MeIm were further studied by ESR spectroscopy as presented below.

ESR Study of the Electrogenerated Iron Tetrapropylporphycenes in the Absence and Presence of N-MeIm. In order to assign the redox site (metal versus ring) as well as the spin state of the different species, i.e. [Fe^{III}TPrPn]Cl, [Fe^{II}TPrPn], $[FeTPrPn]^{\bullet -}$, and $[FeTPrPn]^{2-}$, in the pure solvent or in the presence of excess N-MeIm, the reduced species were generated by electrolysis in the drybox and characterized by their ESR spectra.

The iron(III) species does not display any ESR spectrum at room temperature or at 140 K: High-spin iron(III) complexes usually give observable spectra only at low temperatures[53,54] or broad signals resulting from a high spin or intermediate-spin configurations.[55] In the presence of a large excess of added N-MeIm, a spectrum with lines at $g = 2.43$, 2.27, 2.02, and 1.84, shown in Figure 5, is observed: It is a typical spectrum of low-spin iron(III) complex $[Fe^{III}TPrPn](\text{N-MeIm})_2$[54−58] with an extra line not assigned in the g_x region $g = 2.02$ or $g = 1.84$. In the absence or presence of N-MeIm, the electrogenerated iron(II) species, [Fe^{II}TPrPn], gave no detectable ESR spectra: This is frequently the case with the even-spin iron(II) porphyrins.[54,58−60] The two-electron reduced species $[FeTPrPn]^-$ in the pure solvent gave an ESR spectrum (Figure 6a) displaying two signals at $g = 4.31$ and $g = 2.006$. The line at $g = 4.31$ is of small amplitude and is not common for reduced iron porphyrins and could be ascribed to an impurity.[61] The line at $g = 2.006$ is intense, slightly anisotropic, and very

(51) Collman, J. P.; Reed, C. A. *J. Am. Chem. Soc.* **1973**, *95*, 2048−2049.
(52) Rougée, M.; Brault, D. *Biochemistry* **1975**, *14*, 4100−4106.
(53) Walker, F. A.; Reis, D.; Balke, V. L. *J. Am. Chem. Soc.* **1984**, *106*, 6888−6898.
(54) Yamaguchi, K.; Morishima, I. *Inorg. Chem.* **1992**, *31*, 3216−3222.
(55) Quinn, R.; Nappa, M.; Valentine, J. S. *J. Am. Chem. Soc.* **1982**, *104*, 2588−2595.
(56) Dickinson, L. C.; Symons, M. C. R. *Chem. Soc. Rev.* **1983**, *12*, 387−414.
(57) Otsuka, T.; Ohya, T.; Sato, M. *Inorg. Chem.* **1985**, *24*, 776−782.
(58) Lexa, D.; Momenteau, M.; Mispelter, J. *Biochim. Biophys. Acta* **1974**, *338*, 151−163.
(59) Reed, C. A. *Adv. Chem. Ser.* **1982**, *201*, 333−356.
(60) Yu, B.-S.; Goff, H. M. *J. Am. Chem. Soc.* **1989**, *111*, 6558−6562.
(61) Signals at $g = 4.3$ have been observed in some high-spin peroxoiron(III) porphyrin complexes.[60] The generation of small amounts of peroxoiron(III) through reaction of residual O_2 with iron(II) cannot be ruled out despite the use of an inert-atmosphere box and thus could explain the signal observed at $g = 4.3$.

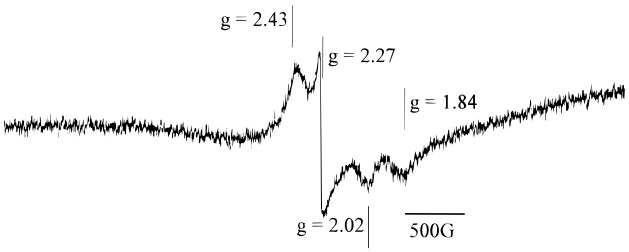

Figure 5. ESR spectrum of $[FeTPrPn]^+$ in PhCN + N-MeIm recorded at 140 K.

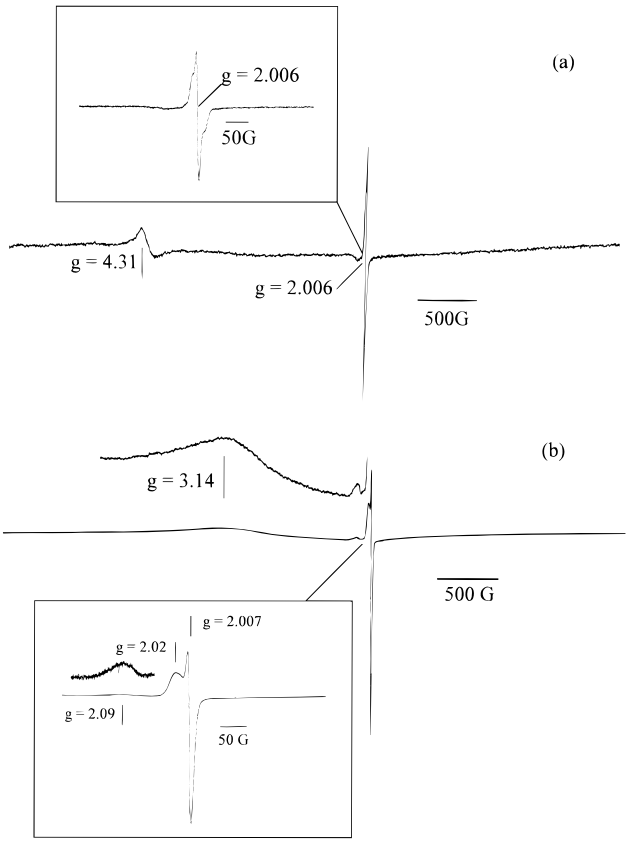

Figure 6. ESR spectra recorded in PhCN at 140 K of the two-electron reduced $[FeTPrPn]^+$ in the absence (a) and in the presence (b) of N-MeIm. Insert: Enlarged central lines.

narrow (ca. 8 G width) and is typical of a π-radical of porphyrins or porphycenes; the two asymmetric side bands at $g = 2.013$ and $g = 1.99$ (insert of Figure 6a) might be indicative of some unpaired spin density on the metal. Indeed, this signal is quite similar to that reported for the π-anion radical of a $Fe^{II}TPP$ derivative.[62] In the presence of added N-MeIm (Figure 6b), the π-anion radical line is much more intense ($g = 2.007$) and is always anisotropic, indicating that the π-anion radical configuration is retained even in the presence of N-MeIm. In this solution condition, the $g = 4.3$ line has disappeared and three new broad lines at $g = 3.14$, $g = 2.09$, and $g = 2.02$ are observed. These could correspond to the species generating the signal at $g = 4.31$ but in the presence of N-MeIm.

In any solution condition, these signals are quite different from those reported for iron(I) porphyrins either axially symmetric ($g_\perp \approx 2.2-2.3$, $g_\parallel \approx 1.90$) or rhombic ($g_x \approx 2.0-2.4$, $g_y \approx 1.9-2.2$, $g_z \approx 1.9-2.0$)[54,62−65] while the typical line of the π-anion radical is observed. This clearly establishes that

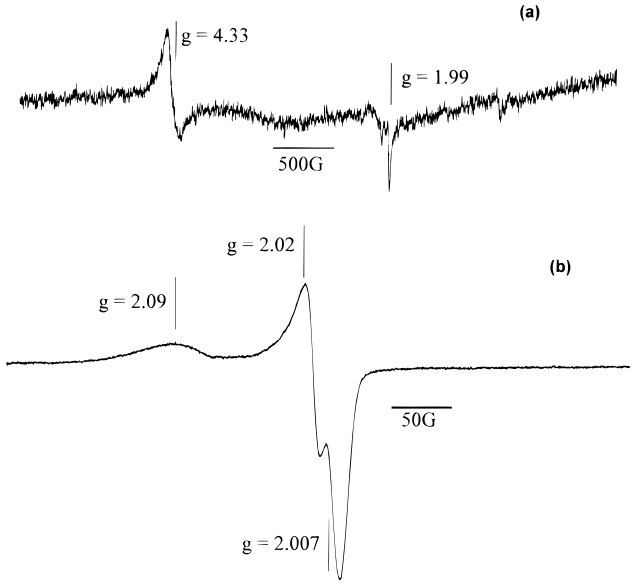

Figure 7. ESR spectra recorded in PhCN at 140 K of the three-electron reduced $[FeTPrPn]^+$ in the absence (a) and in the presence (b) of N-MeIm.

$[Fe^{II}TPrPn^{\bullet}]^-$ is the formulation for the two-electron reduced species.

It should be noted here that, for the two-electron reduced species, a color change occurred when freezing the solution. The solution turned from red-violet at room temperature to green at 140 K. The color change was reversible, and warming the sample regenerated the initial color. Such thermochromism has been described previously for porphyrins[66,67] and could be due to spin-state changes with temperature[68] or solvation changes. The color change occurred only in the solid state (PhCN glass) and could not be followed by UV−vis spectroscopy.

The $[Fe^{II}TPrPn]^{2-}$ species could not be generated quantitatively by bulk electrolysis as mentioned above. The recorded ESR spectra (Figure 7a,b) for the ca. 2.7-electron reduced solution shows that this third reduction step leads to a loss of the π-anion radical line at $g = 2.006$. In the absence or in the presence of N-MeIm the lines at either $g = 4.33$ or $g = 2.09$ and $g = 2.02$, respectively, are retained. As none of these signals are ascribable to $[Fe^{I}TPrPn^{\bullet}]^-$, likely indicating the presence of the same impurity as discussed above, it thus seems reasonable to propose that the third electron reduction step of $[Fe^{III}TPrPn]]Cl$ yields the dianion Fe(II) derivative $[Fe^{II}TPrPn]^{2-}$. Such an assignment is also in agreement with UV−vis spectroscopy, insofar as the absence of any absorbency bands above 450 nm has been demonstrated to be characteristic of the free-base porphycenes dianions and metalloporphycene dianions.[21]

From these results, it can be concluded that, in the case of iron(III) porphycenes, after reduction of the metal to iron(II), the reduction steps are ligand-centered generating the iron(II) anion radical and the dianion, in contrast to iron porphyrins.

(62) Donohoe, R. J.; Atamian, M.; Bocian D. F. *J. Am. Chem. Soc.* **1987**, *109*, 5593−5599.
(63) Cohen, I. A.; Ostfeld, D.; Lichtenstein, B. *J. Am. Chem. Soc.* **1972**, *94*, 4522−4525.
(64) Mashiko, T.; Reed, C. A.; Haller, K. J.; Scheidt, W. R. *Inorg. Chem.* **1984**, *23*, 3192−3196.
(65) Rodgers, K. R.; Reed, C. A.; Su, Y. O.; Spiro, T. G. *Inorg. Chem.* **1992**, *31*, 2688−2700.
(66) Mori, Y.; Sasaki, M.; Daian, C.; Yamada, S. *Bull. Chem. Soc. Jpn.* **1992**, *65*, 3358−3361.
(67) Tsukahara, K.; Tsunomori, M.; Yamamoto, Y. *Inorg. Chim. Acta* **1986**, *118*, L21−L22.
(68) Kambara, T. *J. Chem. Phys.* **1979**, *70*, 4199−4206.

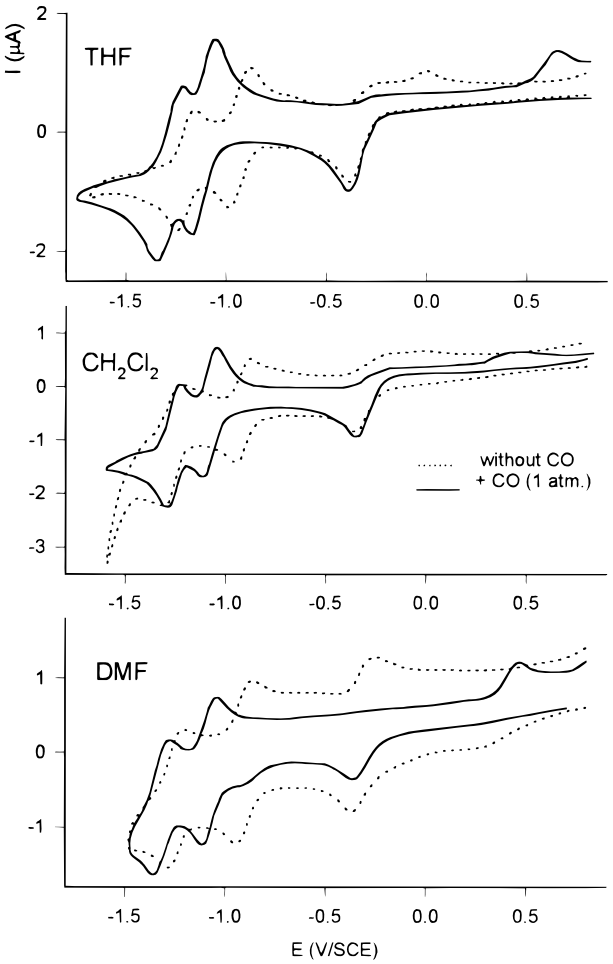

Figure 8. Cyclic voltammetry recorded on Pt at 0.1 V s^{-1} of $[FeTPrPn]^+$ in the absence (dotted line) and in the presence (full line) of CO in different solvents.

Consequently, the porphycene ligand stabilizes iron(II). These results led us to investigate the redox behavior of axially coordinated iron porphycene.

Electrochemical and Spectroscopic Behavior of Axially Coordinated Iron Porphycenes. Redox Behavior [Fe^{III}TPrPn]Cl in the Presence of CO. Cyclic voltammograms of [Fe^{III}TPrPn]Cl in the presence and absence of CO were recorded in THF, CH_2Cl_2, and DMF. As seen in Figure 8 in all the solvents the first reduction step becomes electrochemically irreversible in the presence of CO due to the large affinity of the generated Fe(II) toward CO. The Fe(II)−CO complex is reoxidized at more positive potential as evidenced by an irreversible oxidation peak at $E_p = +0.10$ V vs Fc in THF, −0.03 V vs Fc in DMF, and −0.04 V vs Fc in CH_2Cl_2 for $\upsilon =$ 0.1 V/s. Such a behavior is commonly observed with iron porphyrins.[13,14,33,34] The second reduction step, due to the stabilization of Fe(II) by CO binding, is shifted toward more negative potentials as also observed in porphyrins. It has to be mentioned here that for superstructured iron porphyrins a negative shift of the third reduction step has also been observed, and attributed to CO coordination to Fe(I);[36] however this latter shift was of smaller magnitude and the reversibility was not as well defined as in the present case. Unprecedentedly, as compared to porphyrins, except in dichloromethane, the third reduction step is also shifted to more negative potentials in the presence of CO: −85 mV in THF and −70 mV in DMF. As demonstrated above by ESR and UV−vis spectroscopy, iron in porphycenes is not reduced to iron(I) (although that is commonly observed in porphyrins) but remains as iron(II) which

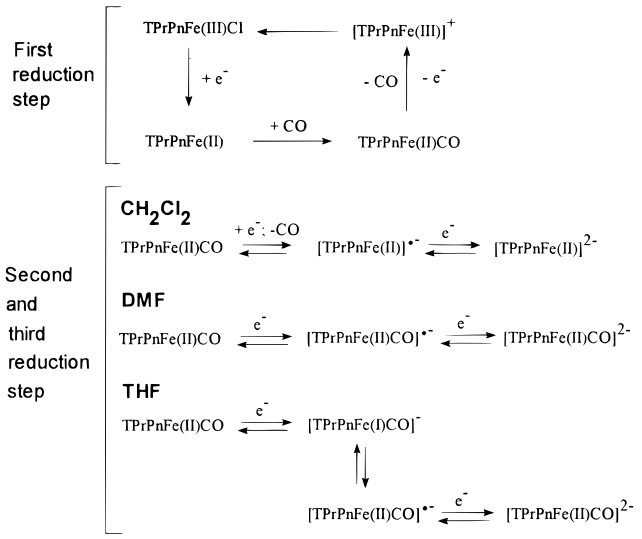

Figure 9. Reduction mechanism of $[FeTPrPn]^+$ in the presence of CO in different solvents.

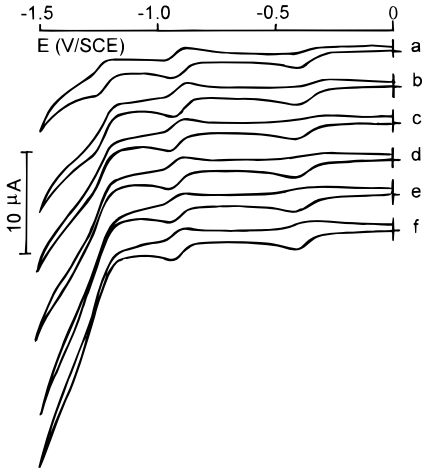

Figure 10. Cyclic voltammetry on Pt at 0.1 V s^{-1} of $[FeTPrPn]^+$ for different partial pressures of CO_2 recorded in CH_2Cl_2 + 0.1 M (TBA)-PF_6: (a) 0 atm; (b) 0.09 atm; (c) 0.21 atm; (d) 0.45 atm; (e) 0.75 atm; (f) 1 atm.

is still able to coordinate CO even in $[Fe^{II}TPrPn]^{2-}$. Spectroelectrochemical studies on platinum OTTLE demonstrate clearly that the spectrum of the generated iron(II) dianion, in the presence of CO differs from that obtained in the absence of CO, as confirmed by the characteristics of the absorption bands reported in Table 2.

In CH_2Cl_2, the redox behavior is similar to iron porphyrins. The observed lack of CO coordination in CH_2Cl_2 is probably due to the low stability of the complexed iron(II) dianion with CO in noncoordinating solvents. It is known that even a weak interaction (with a molecule of solvent for example) at the trans position provides a stronger Fe−CO bond.[52] The absence of the trans coordination in noncoordinating solvent could explain the observed results.

In DMF, in the presence and absence of CO, the spectra of the generated species are different than in CH_2Cl_2, and it is clear, from the redox behavior and from spectral data, that CO remains bound to iron(II) porphycene in all the different reduced species.

In THF the behavior is somewhat peculiar. The OTTLE results indicate that the one-electron—namely iron(II)—and the two-electron reduced species still exhibit a Q band at the same wavelength with reduced absorbencies. Therefore, it is not

Table 2. Wavelengths for the Different Species Observed through OTTLE UV−Vis Spectroscopy in Different Solvents during Reduction of $[FeTPrPn]^+$ in the Absence and Presence of CO (sh = Shoulder)

in CH_2Cl_2

	Species	λ_{max} in nm
[FeTPrPn]Cl	initial species	364 614
	after 1F/mole	302 364 404(sh) 564(sh) 616
	after 2F/mole	296 332 342(sh) 378 398 534 680 744 768
	after 3F/mole	332 390(sh) 422 (sh)
[FeTPrPn]Cl + CO	after 1F/mole	296 386 574(sh) 608
	after 2F/mole	294 332(sh) 344 384 408 536 580 678 744 768
	after 3F/mole	334 390 424(sh)

in **DMF**

	Species	λ_{max} in nm
[FeTPrPn]Cl	initial species	366 618
	after 1F/mole	300 352(sh) 368 584(sh) 618
	after 2F/mole	292 344 377 394 532 682 746 770
	after 3F/mole	302 336 368 404 (sh) 414
[FeTPrPn]Cl + CO	after 1F/mole	300 382 566(sh) 616
	after 2F/mole	300 354(sh) 364 550 762
	after 3F/mole	300 330 420

in **THF**

	Species	λ_{max} in nm
[FeTPrPn]Cl	initial species	296 344(sh) 362 584(sh) 614
	after 1F/mole	296 344(sh) 362 584(sh) 610 622
	after 2F/mole	298 344 376 402 416 534 746 768
	after 3F/mole	300 326 344 366 416
[FeTPrPn]Cl + CO	after 1F/mole	294 384 564(sh) 606
	after 2F/mole	294 384 564(sh) 588
	after 3F/mole	294 384 420

excluded that two species are in equilibrium: $[Fe(I)TPrPn]^-$ ↔ $[Fe^{II}TPrPn^{\bullet}]^-$. However, the three-electron reduced species displayed spectra which were different in the presence and in the absence of CO, confirming the coordination of CO to iron(II). In both cases, no absorbencies characteristic of dianions[21] were observed above 420 nm.

These electrochemical and spectroscopic data led us to propose the following reduction scheme for [FeTPrPn]Cl in the presence of CO (Figure 9).

Redox Behavior $[Fe^{III}TPrPn]Cl$ in the Presence of CO_2. The redox behavior of [FeTPrPn]Cl in the presence of CO_2 was studied in CH_2Cl_2 by cyclic voltammetry at 0.1 V/s for different partial pressure of CO_2 and also at various sweep rates for a 1 atm pressure of CO_2. As shown in Figure 10, cyclic voltammetry, at 0.1 V/s in the presence of CO_2, does not exhibit any change for the two first reductions whereas the third reduction step becomes irreversible in the presence of CO_2 and its amplitude increases with the partial pressure of CO_2 (Figure 10). The shape and the evolution are characteristic of an electrocatalytic reduction of CO_2.[69] Cyclic voltammetry under 1 atm pressure of CO_2 was also carried out for sweep rates ranging from 0.01 to 10 V/s. The third reduction step is reversible at sweep rates higher than 1 V/s and is irreversible for sweep rates lower than 1 V/s. Compared to the second electron transfer, the peak current of the third reduction increases. Plotting Ip_c/Ip_t versus $1/v^{1/2}$ (Ip_c stands for the catalytic current and Ip_t for the charge transfer current in the absence of any catalysis) gave a straight line, in agreement with the theoretical behavior expected for an $E_{rev}C$ catalytic reduction process.[69] The kinetics (k_f) of the follow up chemical reaction were determined using the Nicholson method. We found k_f = 10 mol/s. The electron transfer kinetics (k_s) in the absence of CO_2 were also estimated using the Nicholson method by determining $\psi = f(\Delta E_p)$, where $\psi = (D_{ox}/D_{red})^{\alpha/2}k_s/(\pi a D_{ox})^{1/2}$.[70] The calculated k_s value was equal to 0.01 cm/s. Simulation of the catalytic reaction, using the CVSIM program,[71] gave an S-shaped curve similar to the experimental one which confirms the proposed mechanism. Such S-shaped catalytic reduction of CO_2 by iron porphyrins has been observed previously,[42] and the reduction product has been identified as CO.

Due to the high reactivity of the generated species, no exhaustive electrolysis could be made to examine the products of the electrocatalytic reduction of CO_2. However, during cyclic voltammetry from +0.3 to −2.0 V vs Fc, no oxidation peak characteristic of the generation of FeCO was observed either at −0.04 V vs Fc or at −1.58 V vs Fc, indicating that no CO was generated at the electrode during the catalytic reduction of CO_2 through the iron(II) porphycene dianion. In dry media, no catalysis was observed. This suggests that the presence of residual water (a weak acid) in the solvent enhanced this catalytic process. Indeed, it has been observed recently that iron porphyrins in the presence of weak acids catalyzed the reduction of CO_2[72] into carbon monoxide.

Redox Behavior of $[Fe^{III}TPrPn]_2O$. The electrochemical behavior of the iron μ-oxo derivative $[Fe^{III}TPrPn]_2O$ was also

(69) Nicholson, R. S.; Shain, I. *Anal. Chem.* **1964**, *36*, 706−723.

(70) Nicholson, R. S. *Anal. Chem.* **1965**, *37*, 1351−1355.

(71) Gosser, D. K.; Zhang, F. *Talanta* **1991**, *38*, 715−721.

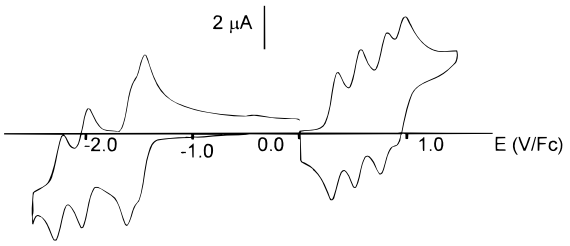

Figure 11. Cyclic voltammetry of $[Fe^{III}TPrPn]_2O$ in dry PhCN + 0.1 M $(TBA)PF_6$ on Pt at 0.1 V s^{-1}.

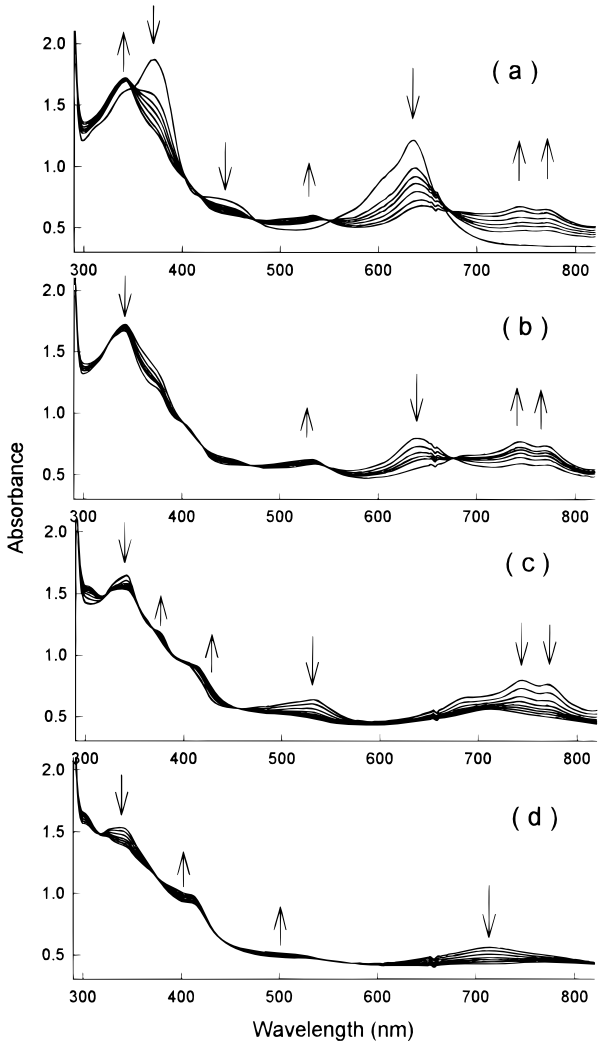

Figure 12. Time-resolved UV−vis absorption spectra of $[Fe^{III}TPrPn]_2O$ in PhCN + 0.1 M $(TBA)PF_6$ on a Pt OTTLE: (a) First one-electron reduction (electrolysis at +0.8 V/Ag); (b) second one-electron reduction (electrolysis at −1.00 V/Ag); (c) third one-electron reduction (electrolysis at −1.3 V/Ag); (d) fourth one-electron reduction (electrolysis at −1.4 V/Ag).

analyzed in dry PhCN. Remarkably, the dinuclear species undergoes eight distinct electron transfers, giving rise to nine different redox states. All of these reactions are reversible one-electron redox processes, as documented in Figure 11. The species is reduced at −1.47, −1.57, −2.00, and −2.24 V vs Fc and oxidized at +0.33, +0.55, +0.79, and +0.95 V vs Fc. Using Pt OTTLE spectroscopy in dry PhCN, it was possible to run, for the first time, all reduction and oxidation processes as shown in Figure 12. The first reduction step of the μ-oxo dimer, $[Fe^{III}$-

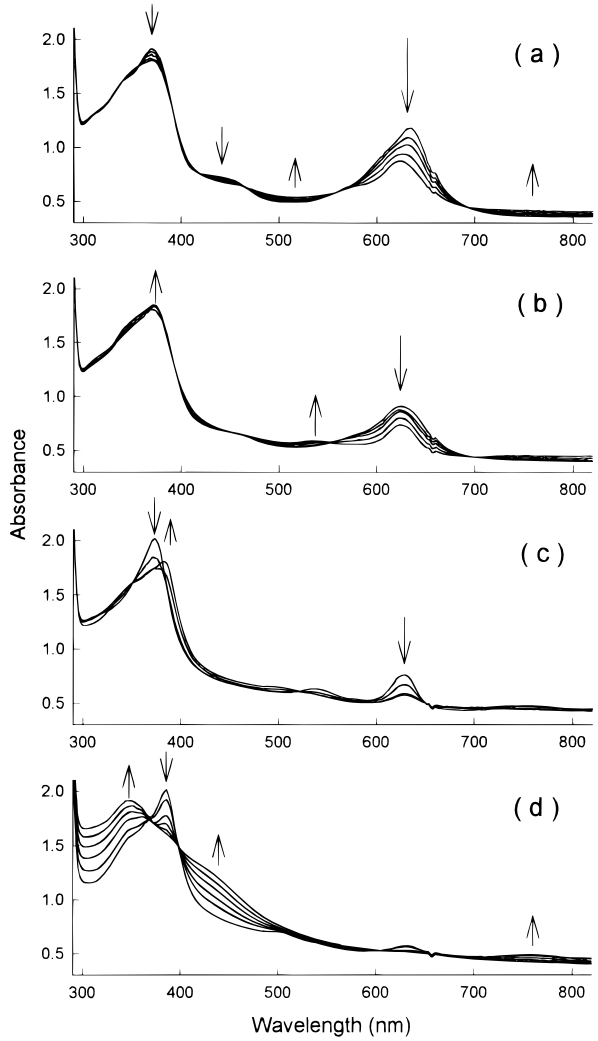

Figure 13. Time-resolved UV−vis absorption spectra of $[Fe^{III}TPrPn]_2O$ in PhCN + 0.1 M $(TBA)PF_6$ on a Pt OTTLE: (a) First one-electron oxidation (electrolysis at +0.8 V/Ag); (b) second one-electron oxidation (electrolysis at + 1.00 V/Ag); (c) third one-electron oxidation (electrolysis at +1.3 V/Ag); (d) fourth one-electron oxidation (electrolysis at +1.4 V/Ag).

$TPrPn]_2O$, yields well-defined isosbestic points at 362, 404, 418, 476, 550, and 670 nm. This is taken as an indication that there are no intermediate chemical species between the starting bis-ferric species and its resulting one-electron reduced form. In contrast to the above, the second reduction step yields an absorption spectrum with bands above 600 nm (Figure 12) typical of anion radicals.[21] However, the spectrum of the direduced species is not identical with that observed for the mononuclear iron(II) radical anion. Thus, it is likely that the dinuclear species is not destroyed during the second reduction step. Further reductions give well-defined isosbestic points at 320, 402, and 452 nm for the third reduction and at 418, 378, 440, and 560 nm for the fourth reduction step. The large decrease of all absorption bands above 400 nm is characteristic of the generation of a dianion on each porphycene ring. Moreover, the initial spectrum of the μ-oxo dimer was restored after stepwise oxidations which demonstrate that the generated species $([Fe^{III}TPrPn]_2O)^{4-}$ is stable on the time scale of the measurements.

Oxidation of the dimer by OTTLE UV−vis spectroscopy led to nice spectroscopic patterns with well-defined isosbestic points for each of the oxidation step (Figure 13). However, in contrast to the reduction processes, the initial spectrum was only fully

(72) Bhugun, I.; Lexa, D.; Saveant, J. M. *J. Am. Chem. Soc.* **1994**, *116*, 5015−5016.

recovered if the electrolysis potential was not set beyond the second oxidation step. Indeed, after microelectrolysis on the plateau potential of the third and fourth oxidation step, only part of the starting material could be recovered indicating a follow-up chemical reaction involving the generated three-electron oxidized species even in hyper dry media. Examination of the spectra of the generated species shows that the one-electron and two-electron oxidized species gave spectra with a Soret-like band (about the same amplitude as in the initial species) and a Q band. These spectra are very different from those recorded during the oxidation of $[FeTPrPn]^+$, shown in Figure 2, which suggests a metal centered oxidation yielding a bis(iron(IV)) species. Identification of the generated oxidized species by ESR failed as the coulometric oxidation could not be carried out without noticeable degradation of the oxidized species. Further oxidation yields spectra with no absorbency above 600 nm characteristic of cation radicals as observed for the free-base porphycene or nickel porphycenes.[21]

Discussion

The present results offer insights into several original properties of iron porphycenes as compared to iron porphyrins. The first striking feature is the formation of stable reduced iron(II) porphycenes, namely the iron(II) radical anion and the iron(II) dianion. The comparison of the redox potentials of porphycenes and porphyrins in CH_2Cl_2 gives the following: (i) for FeTPPCl, −0.77 and −1.55 V (Fe^{II}/Fe^{I} couple) and −2.11V vs Fc and for [FeTPrPn]Cl −0.82 V (Fe^{III}/Fe^{II} couple) and −1.41V and −1.79 V vs Fc; (ii) for H_2TPP, −1.68 V and −2.03 vs Fc and for H_2TPrPn −1.47 and −1.82 V vs Fc. Comparison of these values clearly shows that the redox potential differences between the first and second reductions are nearly equal (ca. 350 mV) in the free-base porphycene and between the second and third reductions in the iron(III) porphycene. This is a common criterion for a electron transfer on the ligand,[9] in full agreement with the above redox site assignments. These values also indicate clearly, as observed previously, that the porphycene ring is reduced at less negative potentials than the porphyrin ring. This feature likely results from lowering of the LUMO energies of the porphycene system as compared to porphyrins. This is proposed to induce a crossing of the metal and ligand orbitals, making the ring levels more accessible for incoming electrons. This effect rationalizes the inversion in reduction sites presently described for the iron derivatives, the second and third reductions being metal centered in the porphyrin and ligand centered in porphycenes. Such redox site tuning has been previously observed in substituted porphyrins bearing an electron-withdrawing group on the meso position or on the β position.[14] Such substituents yield a lowering of the LUMO ring level leading to a change of the reduction site from the metal to the ligand.

This situation also provides a rationale for the unexpected reactivity of the reduced forms of iron porphycenes, especially toward axial ligation. The iron(II) dianion evidenced in the present work is still able to coordinate CO in DMF and THF: This is unprecedented in the literature. This behavior is fully consistent with the proposed generation of the iron(II) dianion, as it is known that iron(I) is a poor complexing agent toward CO.[13] The sole observed coordination of CO for the third reduction step in iron porphyrins corresponds to an iron(I) radical anion or formally iron("0") in superstructured porphyrins.[42]

In the (μ-oxo)iron(III) porphycene dimer, the above-reported electrochemical behavior in CH_2Cl_2 was compared with that of the iron(III) porphyrin analog, $[Fe^{III}TPP]_2O$. Previous studies[73−75] demonstrated that $[Fe^{III}TPP]_2O$ is oxidized in three reversible one-electron steps at +0.36, +0.64, and +1.02 V vs Fc. This behavior is not much different from that observed here with $[Fe^{III}TPrPn]_2O$, which undergoes four distinct one-electron oxidations. Although their oxidation behaviors are essentially similar, $[Fe^{III}TPP]_2O$ and $[Fe^{III}TPrPn]_2O$ differ dramatically in the stability of their reduction products. In either CH_2Cl_2[73] or DMF[76] solution, the porphyrin μ-oxo species decomposes rapidly even after the second reduction step, generating ultimately FeTPP and the corresponding anion radical. By contrast, the porphycene-based μ-oxo derivative $[Fe^{III}TPrPn]_2O$ can be reduced in four distinct one-electron steps. The four reductions are reversible on the time scale of cyclic voltammetry, even at slow sweep rates (0.01 V/s), and also through OTTLE spectroelectrochemistry. The resulting species could then be reduced further to yield a species assigned as $[(Fe^{III}TPrPn)_2O]^{4-}$. This is clearly very different from what is observed with porphyrins. However, only μ-oxo−Fe(III) porphyrin dimers bearing four electron-withdrawing cyano groups lowering the LUMO of the ring system exhibit a similar electrochemical behavior: Four reversible reduction waves were observed[77] for ($[FeTPP(CN)_4]_2O$). However oxidation studies failed as the oxidized species were not stable enough. The possibility of generating a bis(iron(IV)) at a rather low potential is perhaps not negligible as the reduction of iron(III) is very difficult and not observed in our experimental conditions.

Conclusion

This report illustrates a very strong contrast in behavior between iron porphycenes and porphyrins. The difference can be ascribed to an inversion, when comparing porphycene to porphyrin, between the energy levels of the ring LUMO and the metallic orbital. In the case of porphycene, the ring LUMO is lower than the metallic iron orbital making the ring easier to reduce than the metal, in contrast to iron porphyrins. This result yields drastic modifications in the redox properties as well as in the axial reactivity of the iron porphycene compared to porphyrins. The stabilization of reduced forms of iron(II) generates a remarkable reactivity toward axial substrates such as CO at cathodic potentials. This specific behavior is also observed for the (μ-oxo)iron(III) dimer that could be reduced in four reversible one-electron charge transfer steps yielding formally an unexpected stable $[Fe-O-Fe]^{4-}$ (μ-oxo)iron dimer tetraanion at very negative potential, which is unique. These examples illustrate the interest of structural differences, between porphycenes and porphyrins, for the stabilization of uncommon redox intermediates and the exploration of new reaction pathways.

Acknowledgment. The authors thank Prof. E. Vogel for fruitful discussions and continuous interest in their work and for providing them with the iron porphycene samples.

IC970472N

(73) Cohen, I. A.; Lavallee, D. K.; Kopelove, A. B. *Inorg. Chem.* **1980**, *19*, 1100−1101.
(74) Felton, R. H.; Owen, G. S.; Dolphin, D.; Fajer, J. *J. Am. Chem. Soc.* **1971**, *93*, 6332−6334.
(75) Phillippi, M. A.; Goff, H. M. *J. Am. Chem. Soc.* **1979**, *101*, 7641−7643.
(76) Kadish, K. M.; Larson, G.; Lexa, D.; Momenteau, M. *J. Am. Chem. Soc.* **1975**, *97*, 282−288.
(77) Kadish, K. M.; Boisselier-Cocolios, B.; Simonet, B.; Chang, D.; Ledon, H.; Cocolios, P. *Inorg. Chem.* **1985**, *24*, 2148−2156.